Effective High-dose Interferon-α Therapy in a 13-Year-Old Girl With Erdheim-Chester Disease

Ozlem Tezol, MD, Elvan Caglar Citak,† Yavuz Selim Ayhan, MD,* Yuksel Balci, MD,‡ Zehra Pinar Koc, MD,§ and Yasemin Yuyucu Karabulut, MD‖*

Summary: Erdheim-Chester disease (ECD) is a proliferative disorder of non-Langerhans histiocytes with a higher incidence in the fifth to seventh decades and rarer occurrence in the pediatric population. Although ECD typically involves bone, it can also affect the central nervous system, cardiovascular system, retro-orbital space, retroperitoneal space, and kidneys, lungs, and skin. A 13-year-old Syrian girl who presented with multisystemic involvement was diagnosed with ECD. The *B-Raf proto-oncogene V600E* mutation was not detected in ECD lesions. Response to the high-dose interferon-α therapy was excellent in this pediatric patient. In this article, pediatric ECD case reports are also reviewed.

Key Words: child, Erdheim-Chester disease, interferon-α

(*J Pediatr Hematol Oncol* 2020;42:326–331)

Erdheim-Chester disease (ECD) is an uncommon inflammatory disorder with unknown etiology and increasing recognition in the last decade. It is characterized by infiltration of organs and tissues with CD68+, CD1a− non-Langerhans spumous histiocytes. ECD occurs mainly in the sixth decade, more often in male individuals, and, to date, fewer than 20 pediatric cases have been reported.[1,2] Although bone is affected primarily, the clinical spectrum may range from asymptomatic skeletal involvement to multisystemic serious forms. Scientific developments have improved the understanding of the pathogenic mechanisms underlying ECD and therapeutic approaches. B-Raf proto-oncogene (*BRAF*)-*V600E* seems to be crucial in the pathogenesis, *BRAF-V600E* mutation causes activation of the extracellular signal-regulated kinase cellular signaling pathway that is associated with diverse tumors. Langerhans cell histiocytosis and the other non-Langerhans cell disorders are in the differential diagnosis for ECD. In recent years, biologic agents and BRAF-inhibitors have been commonly used for the treatment of ECD.[2,3] In this article, we report a good therapy response to high-dose interferon-α (IFN-α) in a pediatric case presenting with a life threatening, multisystemic form of ECD.

CASE PRESENTATION

A 13-year-old Syrian girl was admitted to the hospital because of fever, fatigue, gait disturbance, respiratory distress, and generalized swelling of 1-month duration. Physical examination revealed bilateral xanthelasmas, edema of the lower extremities, abdominal distension, generalized sclerosis, limitation of joint mobilities, bilateral crepitant rales. The patient was orthopneic, dyspneic, underweight (weight for age < −3 SD), stunted (stature for age < −3 SD), and the stage of puberty was stage 1 according to the Tanner scale. Anemia, C-reactive protein, ferritin, and sedimentation elevation, hypocalcemia, hypophosphatemia, hypomagnesemia, hypoalbuminemia, hypovitaminosis D were abnormal laboratory results (Table 1). Her medical history included excisional biopsy of a palpebral lump 1 year prior in Syria, and a histopathologic diagnosis as non-Langerhans cell reticulohistiocytoma. Despite this diagnosis and persistent multiple lumps on the eyelids, she had not gone to doctor check, and she had not received medical care. Contrast-enhanced thoracic computerized tomography (CT)

TABLE 1. Laboratory Values

Hemoglobine (g/dL)	7.2
Leucocyte ($\times 10^3$/μL)	11.04
Platelet ($\times 10^3$/μL)	485.0
Glucose (mg/dL)	61.0
Urea (mg/dL)	18.1
Creatinin (mg/dL)	0.18
Uric acid (mg/dL)	2.78
Sodium (mEq/L)	140.0
Potassium (mEq/L)	4.18
Chloride (mEq/L)	104.0
25(OH) vitamin D (μg/L)	11.85
Calcium (mg/dL)	7.36
Phosphor (mg/dL)	1.74
Magnesium (mg/dL)	1.25
ALP (IU/L)	155.0
AST (IU/L)	38.0
ALT (IU/L)	14.0
LD (U/L)	530.0
Total protein (g/dL)	5.24
Albumine (g/dL)	2.16
CRP (mg/L)	95.4
Sedimentation (mm/h)	69.0
Ferritine (ng/mL)	689.6
Vitamin B_{12} (pg/mL)	183.0
Folate (ng/mL)	6.06
TSH (μIU/mL)	2.50
FT4 (pmol/L)	15.16
FT3 (pmol/L)	4.84
FSH (IU/L)	0.36
LH (IU/L)	0.07
GH (ng/mL)	1.52
IGF-1(ng/mL)	53.9
ACTH (pg/mL)	16.0
Cortisol (nmol/L)	352.02

ACTH indicates adrenocorticotropic hormone; ALP, alkaline phosphatase; ALT, alanine aminotransferase; AST, aspartate aminotransferase; CRP, C-reactive protein; FSH, follicle-stimulating hormone; FT3, free triiodothyronine; FT4, free thyroxine; GH, growth hormone; IGF-1, insulin-like growth factor 1; LD, lactate dehydrogenase; LH, luteinizing hormone; TSH, thyroid-stimulating hormone.

Received for publication November 16, 2018; accepted May 28, 2019.
From the Departments of *Pediatrics; †Pediatric Oncology; ‡Radiology; §Nuclear Medicine; and ‖Pathology, Faculty of Medicine, Mersin University, Mersin, Turkey.
The authors declare no conflict of interest.
Reprints: Ozlem Tezol, MD, Mersin University Hospital Pediatrics Clinic, Ciftlikkoy Campus, Yenisehir, Mersin 33343, Turkey (e-mail: ozlemtezol@hotmail.com).

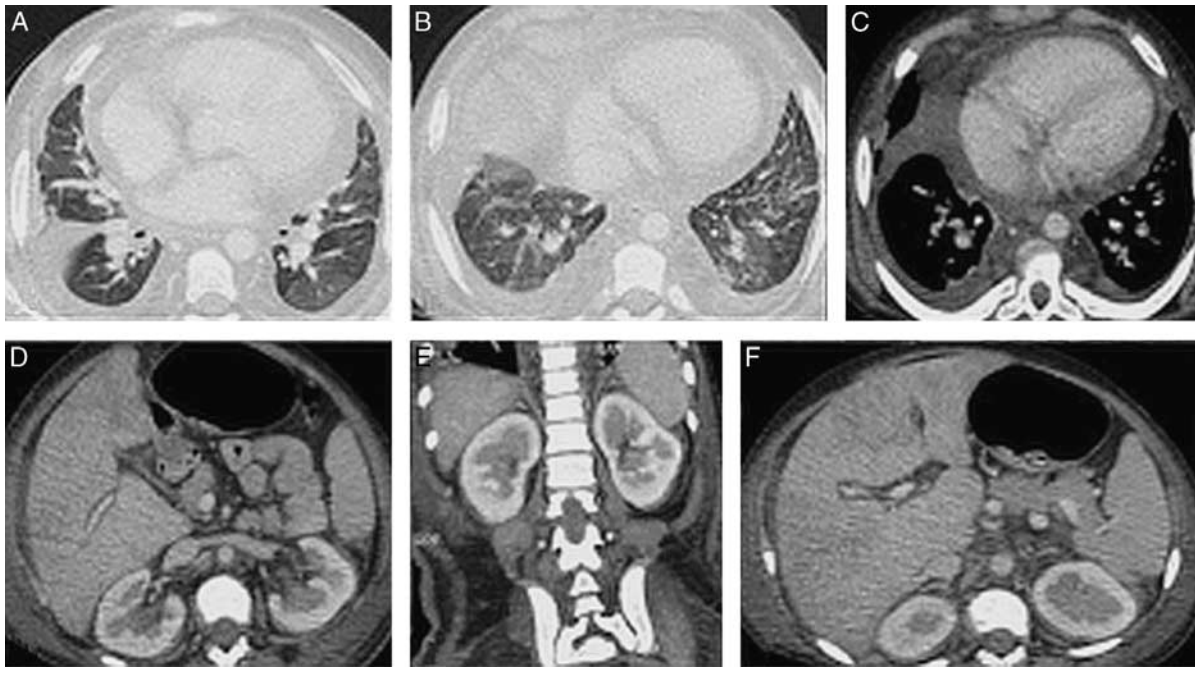

FIGURE 1. Axial contrast-enhanced chest computerized tomography (CT) scan through lung bases shows diffuse smooth symmetric interlobular septal and fissural thickening (A), and diffuse multifocal patchy areas of ground-glass attenuation in bilateral lung bases (B). Mediastinal windowing image shows pericardial and bilateral pleural effusions with thickening (C). Axial and coronal maximum intensity projection reconstruction-enhanced abdomen CT images shows enhancing irregular soft tissue infiltration of the perirenal spaces (hairy kidney appearance) bilaterally (D, E). Abdominal CT image through the liver shows periportal low attenuation (F).

scan showed diffuse smooth symmetric interlobular septal and fissural thickening, and diffuse multifocal patchy areas of ground-glass attenuation in bilateral lung bases, pericardial and bilateral pleural effusions with a thickening. Abdominal CT scan showed enhancing irregular soft tissue infiltration of the perirenal spaces bilaterally and periportal low attenuation, subcutaneous soft tissue edema (Fig. 1). Fluorodeoxyglucose-positron emission tomography/CT images showed increased uptake in the pleural and pericardial thickenings [the maximum standardized uptake value (SUV_{max}) = 3.4], cutaneous and subcutaneous soft tissues of abdomen and legs (SUV_{max} = 4), sacrum and right acetabulum (SUV_{max} = 4.5) (Fig. 2). Radiographs of both arms, forearms, and legs were normal. Echocardiography demonstrated increased pericardial echogenicity and thickness, right heart dilatation, and hepatic veins dilatation. Cerebral, orbital, and pituitary magnetic resonance imagings (MRIs) were normal. Luteinizing hormone, follicle-stimulating hormone, and insulin-like growth factor 1 levels were low, thyroid-stimulating hormone, thyroxine, triiodothyronine, adrenocorticotropic hormone, cortisol levels were normal (Table 1), bone age was the same as chronologic age, and height age was delayed in the endocrine examination. The ophthalmologic examination did not reveal papilledema or visual impairment. Histopathologic examination of the skin biopsy specimen revealed infiltration of the dermis by CD68+, CD1a/S100− foamy histiocytes with epidermal ulceration (Fig. 3). *BRAF-V600E* mutation was not detected in the biopsy sample.

Characteristic histologic findings and characteristic skin, pulmonary, perirenal space involvements, endocrine, and cardiovascular findings were diagnostic for ECD in the present patient. We started treatment with a standard dose of IFN-α (9 mIU/wk, 3 mIU 3 times a week). Despite IFN-α, nasal high-flow oxygen, and decongestive therapy, there was no clinical improvement in the beginning. From the 10th day of therapy, we used high-dose IFN-α (18 mIU/wk, 6 mIU 3 times a week). Thereafter, sclerosis and dyspnea improved within a few weeks. In the second week of high-dose therapy, oxygen support was terminated and in the third week, sclerosis regressed prominently, the patient started to walk. In the fourth week of high-dose therapy, she was mobilized with good joint mobilities, and there were no constitutional symptoms anymore. In the third and sixth months of therapy, radiologic images showed regression of pericardial effusion, pleural effusion, pleural thickness, and ascites, subcutaneous thickness, perirenal involvement (Fig. 4). We plan to continue high-dose IFN-α treatment over several years in expectation of full remission.

DISCUSSION

ECD is a proliferative disorder of non-Langerhans histiocytes with a higher incidence in the fifth to seventh decades and rarer occurrence in pediatric cases. The etiopathogenesis of ECD is not fully known, and no genetic, infectious, or malignant background has been defined. It is believed that ECD occurs as a result of an immunomodulatory mechanism, in which proinflammatory cytokines are released by increased proliferation of T helper cells, and consequently, mast cells proliferate and are activated in the involved tissue.[1]

Skeletal involvement causing bone pain is present in ~96% of ECD cases. Symmetrical, bilateral cortical sclerosis is characteristic in the metaphysis and/or diaphysis of the long bones of the lower extremities. Central diabetes insipidus and exophthalmia are the most common nonbone manifestations. Exophthalmos that develops because of the infiltration of the retro-orbital area is often bilateral and observed in 25% of cases.[1] Bone survey screening and orbital MRI of the present patient were normal. Pathologic histiocytes may cause endocrine findings by infiltrating the pituitary gland in the early stages of ECD. Diabetes insipidus and panhypopituitarism are the most common neuroendocrine manifestations.[1] Our patient had short stature, delayed puberty, and gonadotropin insufficiency, insulin-like growth factor deficiency. She did not respond to the growth hormone secretion stimulating test undertaken at the eighth week of treatment. The patient had no polyuria or polydipsia findings and her pituitary MRI was normal.

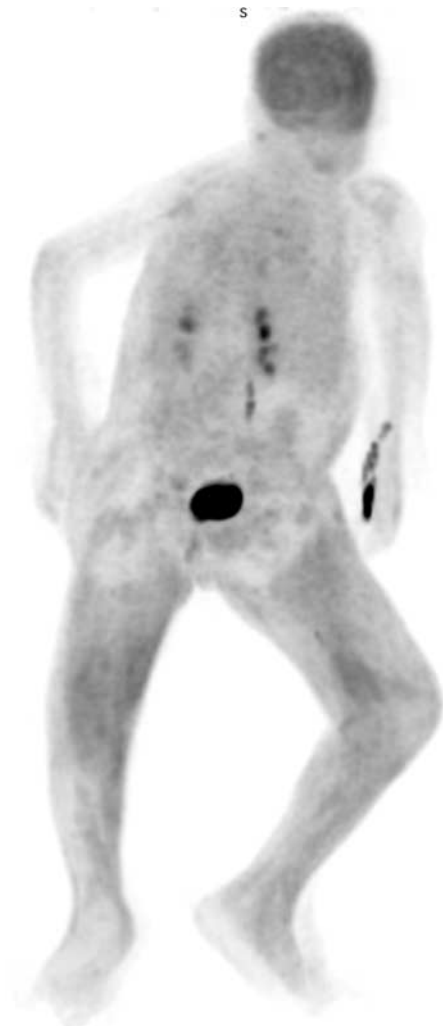

FIGURE 2. FDG-PET scan revealing increased uptake in the pleural and pericardial thickenings, cutaneous and subcutaneous soft tissues. FDG-PET indicate fluorodeoxyglucose-positron emission tomography.

Neurologic involvement responds poorly to treatment and is an independent predictor of mortality. Central nervous system (CNS) involvement is present in approximately half of the cases and leads to death in one third of the cases with this involvement.[1] The brain MRI and ophthalmologic examination of our case were normal. Retroperitoneal space is infiltrated in 30% of the cases and infiltration of perirenal fat tissue leads to the typical "hairy kidney" appearance in abdominal CT as was the case for our patient.[1] Our case presented with urinary tract infection at the time of diagnosis, but we did not observe any urologic complication or nephrovascular hypertension during follow-up. Pulmonary involvement is often asymptomatic, which is important because such involvement worsens the prognosis. In symptomatic patients, as in our case, progressive dyspnea or cough is present. The typical scattered lymphangitic distribution with visceral pleura, interlobular septa, and the bronchoalveolar bundle is observed. In addition to the presence of ground glass opacities and pleural effusion that were also seen in our patient, CT may reveal septal thickening, centrilobular nodules, cysts, and consolidation.[1] Cardiovascular findings are the main cause of mortality in patients with ECD, and ~60% of patients die from cardiac complications. Pericardial involvement develops in 40% to 45% of patients. Pathologic histiocytes may also infiltrate the heart wall, leading to valvular involvement, conduction disorders, and pericoronory invasion.[1] The pericardial effusion, cardiomegaly, and dilatation of the right ventricle and coronary sinus in our patient indicated cardiovascular involvement. However, we did not observe "coated aorta" appearance, which is specific to ECD and occurs as a result of the perivascular infiltration of the thoracic or abdominal aorta. Xanthelasma and xanthomas are the most common skin manifestations of ECD with 30% prevalence.[1] Our patient had bilateral, periorbital, uniformly limited, yellow deposits consistent with xanthelasma. In the second month of treatment, sclerosis on the extremities, abdomen, and back completely disappeared, the xanthelasmas became smaller, there was a reduction in joint immobility, and the patient started to walk with less difficulty. More than 20% of patients diagnosed with ECD have constitutional symptoms, such as fever, weight loss, weakness, and loss of appetite.[4] Our patient's loss of appetite continued until the fourth week of treatment.

The diagnosis of ECD is mainly based on radiologic and pathologic findings. The clinical and radiologic findings of our patient were highly indicative of ECD; therefore, we performed a skin biopsy to confirm the diagnosis. Typical histologic findings include CD68+, CD163+, Factor XIIIa+, CD1a−, S100 −/low, and Langerin foamy histiocytes. A biopsy is also necessary to investigate *BRAF* mutation. *BRAF-V600E* point mutation is identified in >50% of ECD patients.[1] In addition to its oncogenic activity, *BRAF-V600E* mutation has recently been associated with oncogene-induced senescence. It has been hypothesized that *BRAF-V600E* mutant cells can inhibit the transformation of mutant cells into cancer by the local

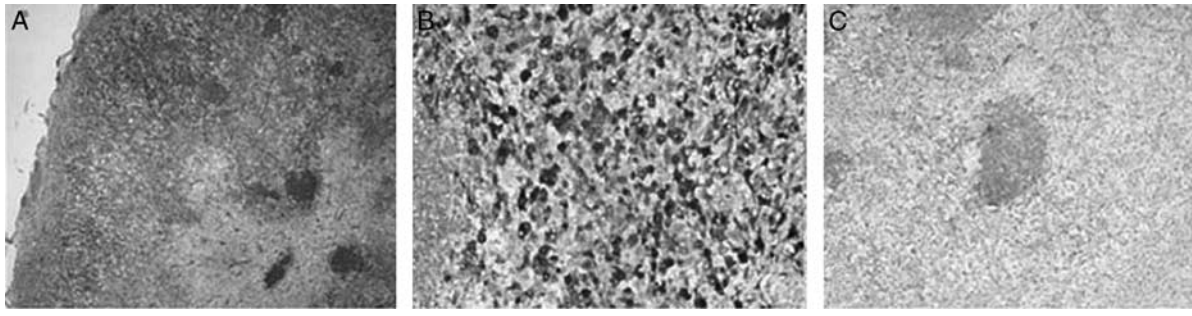

FIGURE 3. Epidermal ulceration with dense dermal histiocyte infiltration (H&E, ×200) (A). Diffuse cytoplasmic positivity with CD 68 (CD68, ×400) (B). CD1a– dermal histiocytes (CD1a, ×200) (C).

Copyright © 2019 Wolters Kluwer Health, Inc. All rights reserved.

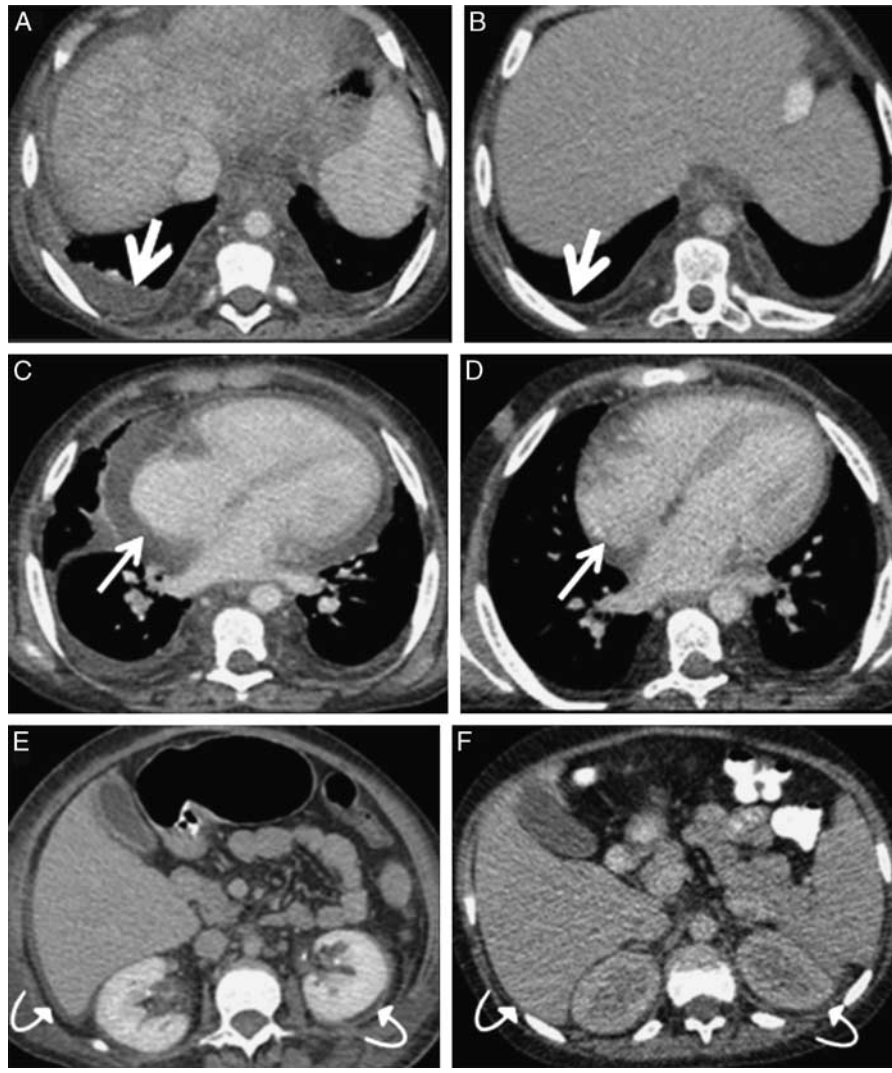

FIGURE 4. Third posttreatment month (A, C, E) and sixth posttreatment month (B, D, F) computerized tomography scans show complete regression of pleural effusions (thick arrows) and pericardial effusions (thin arrows), and partial regression of the soft tissue infiltration in perirenal spaces (curved arrows).

inflammatory reaction, which occurs through the increased production of several cytokines and chemokines.[5] There was no *BRAF* mutation in our case.

For the treatment of ECD, steroids, IFN-α 2a, recombinant human interleukin-1 receptor antagonist, tyrosine kinase inhibitors, bisphosphonates, and cytotoxic agents can be used and autologous hematopoietic stem cell transplantation can be performed. Therapeutic advances have significantly reduced morbidity, but the current 1-year and 5-year survival rates remain relatively high at 96% and 68%, respectively.[1,3]

There are not enough randomized controlled trials investigating different therapeutic approaches in the treatment of ECD.[3] Table 2 presents the clinical features and treatment approaches of some pediatric patients reported in the English literature.[4,6–17]

IFN-α is used in the treatment of histiocytosis because of its immunomodulatory properties. IFN-α has been considered as the first-line treatment for symptomatic ECD since its effectiveness was first reported in 2005.[18] In a cohort study with 46 adult patients, IFN-α or pegylated IFN-α significantly improved survival compared with other treatments. Although the efficacy of IFN-α varies depending on the area of involvement, the minimum required dose is 3 mIU 3 times a week. In severe forms of ECD with CNS or cardiovascular involvement, the recommended dose is 9 mIU 3 times a week.[19] Hervier and colleagues reported that ≥18 mIU dose/week resulted in better treatment response in patients with CNS, pituitary, lung, and cardiac involvement compared with those with bone, ear, nose, and throat involvement. There was no worsening of the vascular, hypophysical, or pulmonary findings of any of their patients. During a median follow-up of 19 months, the authors reported 64% improvement in cases with CNS involvement and 79% improvement in patients with cardiac involvement. Furthermore, the tolerance for standard dose and high-dose IFN-α treatment was similar. The authors suggested that treatment may take a few years, possibly 3 years or longer because of the slow recovery process.[20]

To the best of our knowledge, this is the first case report of ECD in the literature presenting a pediatric patient that underwent high-dose IFN-α treatment because of multisystem

TABLE 2. Pediatric Case Samples With Erdheim-Chester Disease in English Literature

References	Case	Symptoms—Findings	Clinical Manifestation	*BRAF V600E* Mutation	Therapy	Prognosis
Hao et al[6]	11-year-old boy	Intermittent headache and generalized bone pain, palpable scalp masses, exophthalmos, developmental delay Diffuse bone destruction, multiple giant intracranial lesions	Mixed LCH and ECD	Positive in both LCH and ECD lesions	Dabrafenib	Stable condition, no new lesions
Váradi et al[7]	20-month-old boy	Visible soft masses on the left temporal and right parietal bone Destructive frontal and frontotemporoparietal masses, extensive bone marrow and spleen involvement	LCH initially, ECD later on	Positive in both LCH and ECD lesions	Vemurafenib	In the 18th month of therapy ECD is in complete remission
Vallonthaiel et al[8]	6-year-old girl	Pain and swelling in the right upper arm Focal lesions involving maxilla, mandible, left scapula, dorsal vertebra, sacrum, bilateral femur, tibi, and humerus	ECD	Negative	Conservative treatment with anti-inflammatory drug	—
White et al[9]	5-year-old boy	Progressive polyuria, polydipsia, weight loss and abdominal pain Enhancing lesion centered on the hypothalamus and the pituitary stalk, involving the optic chiasm	ECD	—	Steroids, interleukin-1 receptor antagonist (anakinra), vinblastine	In the third month of therapy markedly decreases in lesion enhancement
Kim et al[10]	3-year-old boy	Headache and right exophthalmos Intracranial and skeletal bone lesions	Coexistence of ECD and LCH	Positive in both LCH and ECD lesions	Initially prednisolone, vinblastine, methotrexate, cyclophosphamide, later on cladribine and cytarabine	In the fourth month of therapy a partial response
Alimohamadi et al[11]	14-year-old boy	Hypesthesia and dysesthesia of the first and third branches of the right trigeminal nerve and diplopia Mass in the right cavernous sinus and Meckel cave, extending to the posterior fossa	ECD	—	Cytotoxic and corticosteroid therapy	Under care for 8 y
Song et al[12]	4-year-old boy	Right hemifacial palsy, right shoulder pain, seizure attack Bone, lung, CNS involvement	ECD	—	Interferon α-2b, cyclosporin, and dexamethasone	In the sixth month of therapy near complete improvement of pulmonary involvement and little change of other involvements
Tran et al[4]	10-year-old girl	Recurrent fever, bone pain, and failure to thrive Multiple osteolytic and osteosclerotic lesions in the femurs, tibia, pelvis, and retroperitoneal infiltration	ECD	—	Initially IFN alfa-2a and PEGylated IFN alfa-2a, later on Anakinra	In the seventh month of therapy weight and height gain but no significant changes in the bone lesions or retroperitoneal infiltration
Jeon et al[13]	17-year-old girl	Lumbago, pelvic pain, and pain in both legs, tenderness in the lumbar area and pelvic area Multiple skeletal lesions and areas posterior to the bilateral neck and axillary areas, the mediastinal, paraaortic, inguinal areas, and the spleen involvements	ECD	—	Vinblastine, prednisone, methotrexate, 6-MP combined with IFN-i	Free of any lesions 2 y after the completion of combination treatment

Copyright © 2019 Wolters Kluwer Health, Inc. All rights reserved.

Kumandas et al[14]	10-year-old boy	Gait abnormalities, weakness, cerebellar ataxia, increased deep tendon reflexes, clonus, positive plantar responses CNS, and bone lesions	ECD	—	Steroid 2 mg/kg/d	—
Sohn et al[15]	10-year-old girl	Arthralgias, intermittent fever, weight loss, fatigue Lower legs, hands, forearms, facial bones involvement	ECD	—	High-dose steroids	Still alive after a 32-month follow-up
Joo et al[16]	10-year-old girl	Long bones of the upper and lower extremities involvement	ECD	—	Steroid therapy for 8 mo	Remarkable restoration
Clerico et al[17]	14-year-old girl	Recurrent pain and swelling in both knees, and the elbows, fever, abdominal pain, anemia Bone, omentum, lung, mammary gland, brain	Juvenile xanthogranulom initially, ECD later on	—	Initially treatment according to the LCH-II-stratification, later on 3 cycles of carboplatin plus etoposide, than monthly injections of somatostatin	An indolent course, no progressive lesions and no extraskeletal involvement 33 mo after onset of symptoms

BRAF indicates B-Raf proto-oncogene; CNS, central nervous system; ECD, Erdheim-Chester disease; IFN, interferon-α; LCH, langerhans cell histiocytes.

involvement. After observing no side effects, good treatment efficacy, and good tolerance, we plan to continue the treatment for a few years. High-dose IFN-α therapy may provide improvement or stabilization in pediatric severe ECD cases.

REFERENCES

1. Campochiaro C, Tomelleri A, Cavalli G, et al. Erdheim-Chester disease. *Eur J Intern Med*. 2015;26:223–229.
2. Haroche J, Cohen-Aubart F, Rollins BJ, et al. Histiocytoses: emerging neoplasia behind inflammation. *Lancet Oncol*. 2017;18: e113–e125.
3. Cohen Aubart F, Emile JF, Carrat F, et al. Targeted therapies in 54 patients with Erdheim-Chester disease, including follow-up after interruption (the LOVE study). *Blood*. 2017;130: 1377–1380.
4. Tran TA, Fabre M, Pariente D, et al. Erdheim-Chester disease in childhood: a challenging diagnosis and treatment. *J Pediatr Hematol Oncol*. 2009;31:782–786.
5. Cangi MG, Biavasco R, Cavalli G, et al. BRAFV600E-mutation is invariably present and associated to oncogene-induced senescence in Erdheim–Chester disease. *Ann Rheum Dis*. 2015;74:1596–1602.
6. Hao X, Feng R, Bi Y. Dramatic efficacy of dabrafenib in Erdheim-Chester disease (ECD): a pediatric patient with multiple large intracranial ECD lesions hidden by refractory Langerhans cell histiocytosis. *J Neurosurg Pediatr*. 2018;23: 48–53.
7. Váradi Z, Bánusz R, Csomor J, et al. Effective BRAF inhibitor vemurafenib therapy in a 2-year-old patient with sequentially diagnosed Langerhans cell histiocytosis and Erdheim–Chester disease. *Onco Targets Ther*. 2017;10:521–526.
8. Vallonthaiel AG, Mridha AR, Gamanagatti S, et al. Unusual presentation of Erdheim-Chester disease in a child with acute lymphoblastic leukemi. *World J Radiol*. 2016;8:757–763.
9. White TV, Silvester NC, Otero HJ. Non-sclerotic bone involvement in Erdheim–Chester: PET/CT and MRI findings in a 15-year-old boy. *Pediatr Radiol*. 2016;46:1345–1349.
10. Kim S, Lee M, Shin HJ, et al. Coexistence of intracranial Langerhans cell histiocytosis and Erdheim-Chester disease in a pediatric patient: a case report. *Childs Nerv Syst*. 2016;32: 893–896.
11. Alimohamadi M, Hartmann C, Paterno V, et al. Erdheim-Chester disease mimicking an intracranial trigeminal schwannoma: case report. *J Neurosurg Pediatr*. 2015;15:493–498.
12. Song SY, Lee SW, Ryu K, et al. Erdheim-Chester disease with multisystem involvement in a 4-year-old. *Pediatr Radiol*. 2012; 42:632–635.
13. Jeon I, Lee SS, Lee MK. Chemotherapy and interferon treatment of Erdheim–Chester disease. *Pediatr Blood Cancer*. 2010;55:745–747.
14. Kumandas S, Kurtsoy A, Canoz O, et al. Erdheim Chester disease: cerebral involvement in childhood. *Brain & Development*. 2007;29:227–230.
15. Sohn MH, Kim MW, Kang YH, et al. Tc-99m MDP bone and Ga-67 citrate scintigraphy of Erdheim–Chester disease in a child. *Clin Nucl Med*. 2006;31:90–92.
16. Joo CU, Go YS, Kim IH, et al. Erdheim-Chester disease in a child with MR imaging showing regression of marrow changes. *Skeletal Radiol*. 2005;34:299–302.
17. Clerico A, Ragni G, Cappelli C, et al. Erdheim–Chester disease in a child. *Pediatr Blood Cancer*. 2003;41:575–577.
18. Braiteh F, Boxrud C, Esmaeli B, et al. Successful treatment of Erdheim-Chester disease, a non-Langerhans-cell-histiocytosis with interferon-alpha. *Blood*. 2005;106:2992–2994.
19. Haroche J, Amoura Z, Trad SG, et al. Variability in the efficacy of interferon-alpha in Erdheim-Chester disease by patient and site of involvement: results in eight patients. *Arthritis Rheum*. 2006;54:3330–3336.
20. Hervier B, Arnaud L, Charlotte F, et al. Treatment of Erdheim-Chester disease with long-term high-dose interferon-α. *Semin Arthritis Rheum*. 2012;41:907–913.